Development of Multiwalled Carbon Nanotube Integrated Field Effect Transistor for Highly Sensitive HIV-1 Tat Protein Biosensor

by

Fatin Nabilah Mohd Faudzi
(1441711273)

A thesis submitted in fulfillment of the requirements for the degree of Doctor of Philosophy

Institute of Nano Electronic Engineering
UNIVERSITI MALAYSIA PERLIS

2019

ACKNOWLEDGMENT

Alhamdulillah, praise to Allah, the Almighty and Merciful, for His grace has enabled me to complete my thesis hence concluded my PhD journey. It was an individual journey that was accomplished with strong supports from people around me.

This thesis would not come to an existence without the kind guidance from my supervisor, Dr. Ruslinda A. Rahim. She is indeed a great mentor that has taught me to do my best, be positive and confident in my research. It was her patience and strong support that kept lifting me through tough times. Many thanks to Dr. Mohd Khairuddin Md Arshad, my co-supervisor for his knowledge sharing and guidance. My gratitude also goes to Dr. Subash Gopinath, for his kind heart and willingness to help me in my research.

I have my family to thank to for giving me a chance to pursue knowledge during these five long years. It was my late father, Mohd Faudzi Bakar that always encourages me to pursue my study and my dreams. Thank you Ayah, for being the best father for me. My deepest appreciation goes to my mother, Fairuz Abdullah for being understanding and supportive through this overwhelming journey. Thank you for your trust and patience. Along and Abang, thank you for giving me an opening to pursue my study and took up the responsibility towards family which should be mine to share with. Farah, Amin, Adik and Acu, thank you for just being my family and make me happier in a lot of ways.

My gratitude also goes to INEE lecturers, admin and lab staffs, late Mr. Aizat, Mr. Jasni, Mrs. Mira and others whom directly or indirectly have shared their knowledge and opinions and helped me with my research work. Your assistances are much appreciated. My dear labmates, Lee Hon Cheun, Adzhri, Conlathan, Faris, Iman, Adelyn, Adila, Atiqah, Azizah, Farehanim, Huda, Humaira, Khairun , Nasyifa, Thivina and others, thank you for all the time we spent together. Your friendship and love are the memories that I will seize for a lifetime.

Finally, thank you to Prof. Richard Jackman, Diamond Electronic Group and Kak Azie and Abang Nasrun's family. All of you have alleviated my life in the foreign country. The attachment opportunity was a precious experience that I can never forget, that has made me grew mature in some aspect of life.

TABLE OF CONTENTS

		PAGE
DECLARATION OF THESIS		**i**
TABLE OF CONTENTS		**iii**
LIST OF TABLES		**vi**
LIST OF FIGURES		**vii**
LIST OF ABBREVIATIONS		**xiv**
LIST OF SYMBOLS		**xvii**
ABSTRAK		**xx**
ABSTRACT		**xxi**
CHAPTER 1 :	**INTRODUCTION**	**1**
1.1	Background	1
1.2	Research Problem Statement	5
1.3	Research Objectives	8
1.4	Research Scope	9
1.5	Thesis Organization	11
CHAPTER 2 :	**LITERATURE REVIEW**	**12**
2.1	Biosensor	12
2.2	Types of biosensor	14
2.3	Field effect transistor: An electrochemical biosensor	17
2.4	Nanotechnology: Nanomaterials in electrochemical biosensor device	20
2.4.1	Multiwalled carbon nanotube	22

2.5 Covalent surface functionalization of carbon nanomaterials 24

2.6 Carbon nanomaterial – FET integration method 27

2.7 Antibody and aptamer as sensing probe 30

2.8 Sensing probe immobilization method on biosensor 33

2.9 Biosensor as HIV detection device 35

2.9.1 Current HIV detection method 38

2.9.2 Target protein for biosensor – HIV-1 Tat 40

2.9.3 HIV-1 Tat protein biosensor 46

2.10 Colorimetric assay as biosensor validation method 51

2.11 Summary of material and method selection 52

CHAPTER 3 : METHODOLOGY 55

3.1 Introduction 55

3.2 Back gate field effect transistor device fabrication 56

3.3 Multiwalled carbon nanotube – back gate field effect transistor integration 59

3.3.1 MWCNT functionalization and characterization 60

3.3.2 MWCNT deposition study 63

3.4 HIV-1 Tat detection by immunoassay method 65

3.4.1 Biomolecules purity validation 65

3.4.2 Colorimetric assay 66

3.5 HIV-1 Tat detection by electrical method 67

CHAPTER 4 : RESULTS & DISCUSSION 69

4.1 Introduction 69

4.2 Back gate field effect transistor device fabrication 69

4.3 Multiwalled carbon nanotube – back gate field effect transistor integration 72

4.3.1 MWCNT functionalization and characterization 72

4.3.2 fMWCNT deposition on BGFET device 87

4.3.3 fMWCNT – BGFET device performance 92

4.4 HIV-1 Tat protein detection approach 95

4.4.1 HIV-1 Tat detection by immunoassay method 96

4.4.1.1 Biomolecules purity validation 96

4.4.1.2 Colorimetric assay 97

4.4.2 HIV-1 Tat detection by MWCNT – BGFET 107

CHAPTER 5 : CONCLUSION 117

5.1 Introduction 117

5.2 Conclusion 117

5.3 Future works 122

REFERENCES 125

APPENDIX A CALCULATION DETAILS 144

APPENDIX B LIST OF PUBLICATIONS 146

APPENDIX C LIST OF AWARDS 156

LIST OF TABLES

		PAGE
Table 2.1	Types of HIV-1 protein (Frankel & Young, 1998).	43
Table 2.2	HIV-1 Tat protein detection (Fatin et al., 2016)	49
Table 3.1	MWCNT functionalization method.	61
Table 4.1	Percentage of fMWCNT weight loss at different temperature range.	78
Table 4.2	MWCNT dispersion in IPA.	81
Table 4.3	Carbon peak fitting for MWCNT and fMWCNT.	87
Table 4.4	Oxygen peak fitting for MWCNT and fMWCNT.	87
Table 4.5	Measured thickness of sprayed fMWCNT.	90
Table 4.6	Conductance value of the deposited fMWCNT.	91
Table 5.1	HIV-1 Tat protein detection	120

LIST OF FIGURES

		PAGE
Figure 1.1	Schematic diagram of BGFET for DNA/protein biosensor.	3
Figure 1.2	Flow chart of the HIV-1 Tat sensor development process	10
Figure 2.1	Components in biosensor (Hendry, Higgins, & Bannister, 1990).	13
Figure 2.2	Biosensor classified according to their sensing probes (Preda, Bizerea, & Vlad-oros, 2011).	14
Figure 2.3	Biosensor classified according to their transducers (Preda et al., 2011).	15
Figure 2.4	Label-free and label-based biosensor (Sang, Zhang, & Zhao, 2013).	17
Figure 2.5	Basic BGFET figure (Z. Zhu, 2017).	18
Figure 2.6	SGFET detection mechanism. (a) Addition of target protein and (b) regeneration (removal of target) using urea solution. The difference in the current curve after biomolecule immobilization and detection is due to the difference in charge on the channel surface. The changes of the signal are recorded as (i) the curve recorded for the immobilized sensing probe on SGFET and (ii) the reduction in current was due to the positive charge from the target protein. After the regeneration process, the current curve will shift back to the initial condition as in (i) (Ruslinda et al., 2013).	19

Figure 2.7 Carbon nanotubes looks like a rolled graphene sheet. Figure shows three structures of (a) graphene sheet, (b) SWCNT and (c) MWCNT (Kreupl et al., 2002) 23

Figure 2.8 Sensing probe based detection (a) antibody based detection; (b) aptamer based detection. These sensing probes display different affinities. Other differences between these sensing probes are stability and suitable for chemical modification. 33

Figure 2.9 Steps of HIV regulation in infected cells. (1) Viral fusion with the host cell, (2) release of HIV proteins and RNA into the host cell, (3) viral RNA is carried across the nuclear membrane, (4) viral RNA integration into host DNA, (5) production of new viral proteins, (6) formation of new viruses on the cell surface and (7) release of individual viruses. The function of HIV-1 Tat protein is needed between steps no. 4 and 5 during the transcription of new viral RNA (Suzuki & Suzuki, 2011). 37

Figure 2.10 Schematic reaction of a lateral flow system (a) before analytes pass through the strip and (b) after analytes pass through the strip. When analytes pass through the strip, they bind to the conjugated antibody at the conjugate pad, and the complex will bind an antibody immobilised on the test line. The unbound conjugated antibody will bind to the specific antibody on the control line. This type of reaction will produce two coloured bands on the strip (positive reaction), indicating the present of the analyte in the sample solution (Bahadır & Sezgintürk, 2016). 40

Figure 2.11 Structure of human immunodeficiency virus with a diameter of approximately 120 nm (Kirchhoff, 2013). 41

Figure 2.12 (a) HIV-1 Tat protein region (Tombelli, Minunni, Luzi, & Mascini, 2005) and (b) the protein structure based on its

region by colour difference (Protein Data Bank accession code 1TIV). 45

Figure 2.13 This schematic illustrates the (a) mechanism of GNP and NaCl salt. NaCl causes GNP to aggregate and changes its color from red to purple. During interaction of GNP, DNA strand and NaCl in (b), GNP does not change colors since DNA strands adsorbed to its surface prevents interaction with NaCl. While in (c), target molecule added to the mixture causes DNA strand to leave GNP and bind with its target, hence GNP react with NaCl and changes color to purple (Gopinath et al., 2014). 52

Figure 3.1 Experimental work flow. 55

Figure 3.2 Layers in SOI wafer. 56

Figure 3.3 FET device fabrication scheme. (i) Preparation of SOI wafer, (ii) PR coating and photolithography process (first mask), (iii) Top silicon layer etching by RIE, (iv) SiO_2 removal using BOE, (v) Ni/Au deposition by metal evaporator, (vi) PR coating and photolithography process (second mask), and (vii) Ni/Au etching to form source (S), drain (D) and gate (G) electrode. 58

Figure 3.4 MWCNT deposition on substrate by using a spray method. 64

Figure 3.5 The electrical measurement of FET was conducted using two sourcemeter forming a three electrode measurement setting. 65

Figure 4.1 Photolithography proves on SOI wafer for device fabrication. (a) The SOI wafer was cut into small pieces, (b) The cleaned wafer was coated with PR, (c) The PR has been exposed under UV light and developed into desired pattern, (d) Image of the 100 μm FET channel under HPM. 70

Figure 4.2 Image of (a) Fabricated BGFET device and (b) Schematic diagram of the BGFET 72

Figure 4.3 FTIR spectrum of MWCNT and fMWCNT that was overlapped showing the presence of new peak at 1750 cm^{-1} which indicates the presence of carboxyl functional group after functionalization treatment in mild acid mixture. 75

Figure 4.4 Morphological characterization using SEM shows the image of (a) MWCNT and unharmed structure of fMWCNT after mild acid treatment using Method I (b) and Method II (c). 76

Figure 4.5 Analysis using TGA showing the weight loss percentage of MWCNT and fMWCNT. 78

Figure 4.6 Dispersion test shows that (a) Unfunctionalized MWCNT or under functionalized MWCNT precipitate to the bottom of the container in less than 24 hours while (b) Functionalized MWCNT dispersed uniformly in the solvent. 80

Figure 4.7 The XRD result displays the similar profile pattern of MWCNT and fMWCNT. This indicates that the functionalization treatment is a mild oxidation method and introduces no major defect on the MWCNT surface. 83

Figure 4.8 FESEM image of MWCNT (a) normal and (b) enlarged and fMWCNT (c) normal and (d) enlarged. 83

Figure 4.9 The XPS surface characterization reveals the increase in oxygen content after functionalization treatment as in the survey spectra in (a). Carbon peak fitting for (b) MWCNT and (c) fMWCNT, shows a decrease in carbon intensity whereas an increase in oxygen intensity indicates the formation of the additional oxygenated functional group. Oxygen peak fitting of (e) MWCNT and (f) fMWCNT

shows an increase of nearly six folds of the peak intensity after functionalization. 85

Figure 4.10 fMWCNT deposited via spray method using (a) 0.2 ml, (b) 0.4 ml and (c) 0.8 ml fMWCNT solution.It has been characterized under SEM showing increase in density of fMWCNT network deposited. 89

Figure 4.11 (a) The current-voltage measurement of deposited fMWCNT layers. (b) The conductivity value of different fMWCNT solution volume deposited. 91

Figure 4.12 SEM image of deposited fMWCNT on BGFET. 92

Figure 4.13 Illustrated MWCNT layer deposited on BGFET device channel. 93

Figure 4.14 Characterization of fMWCNT-FET device shows (a) The I_{ds}–V_{ds} result at multiple gate voltage supplied (-1 V, -0.5 V and 0 V). Schematic in (b) shows the working principle occurring in the device. (c) The I_{ds}–V_{gs} result at multiple drain voltage supplied (-1 V, -0.5 V and 0 V). 94

Figure 4.15 PAGE analysis of (a) RNA aptamer S1, (b) RNA aptamer S2, and (c) Recombinant HIV-1 Tat protein. 97

Figure 4.16 Interactions of split RNA aptamer with cognate molecule HIV-1 Tat. The binding of both strands is stabilized in the presence of HIV-1 Tat. Strand 1 is 16 mer, and Strand 2 is 19 mer. The crystal structure of HIV-1 Tat is shown in Bayer *et al*. (1995) (P. Bayer et al., 1995). 98

Figure 4.17 (a) Colorimetric analysis of NaCl titration of GNP showing color transition from red to purple with increasing concentration of NaCl, (b) Peak shifting can be observed with UV-Vis spectrum during NaCl titration of GNP concurrent with the changes of color. 100

Figure 4.18 FESEM image of (a) GNP, (b) GNP agglomeration with 250 mM of NaCl. 102

Figure 4.19 Aptamer concentration detection conducted before LOD detection has indicated that 50µM of split RNA aptamer S1 is needed to prevent GNP aggregation with salt solution. 103

Figure 4.20 Specificity analysis of HIV-1 proteins against the split RNA aptamer. HIV-1 Tat, P24, and Nef were tested. (a) Schematic reaction between aptamer and protein, (b) HIV-1 proteins-aptamer complex in GNP solution show transition of color from red to purple, (c) The spectral shift with the presence of Tat has shown the furthest shift among all HIV protein tested. 104

Figure 4.21 Determination of the sensitivity. (a) Spectral changes in the absence of HIV-1 Tat. (b) Changes in the absorbance in the absence of HIV-1 Tat. (c) Spectral changes in the presence of HIV-1 Tat. (d) Changes in the absorbance in the presence of HIV-1 Tat. The background with non-specific values was determined and indicated by broken lines. 106

Figure 4.22 Zero-length crosslinking reaction mechanism of carboxyl functional group from fMWCNT and amine functional group from RNA aptamer S1. This reaction will provide stable amine reactive NHS intermediate that will leave the fMWCNT surface once amine is present in the reaction. 108

Figure 4.23 Schematic of BGFET channel surface after chemical and biological treatments showing (a) fMWCNT on BGFET channel with carboxylated functional group on surface, (b) Amine-reactive NHS intermediate on fMWCNT after EDC/NHS treatment, (c) RNA aptamer S1 immobilized as probe, (d) Ethanolamine blocking treatment to mask the unreacted amine-reactive NHS intermediate site and (e)

HIV-1 Tat intercalation on strand 1 aptamer probe with RNA aptamer S2. 109

Figure 4.24 FTIR characterization of binding formed during biomolesules interaction. 110

Figure 4.25 Electrical characterization of HIV-1 Tat protein detection showing (b) The I_{ds}–V_{gs} of the detection process of 10 nM HIV-1 Tat protein showing a shift in gate voltage value at 1 mA current yield after chemical and biological treatments, (c) Enlarged graph of (b) showing gate voltage shift from the fMWCNT-BGFET bare device until Tat protein detection, (d) Gate voltage shift after every detection steps as summarized in (a) were plotted in error bar (n=3). 112

Figure 4.26 Specificity test of HIV proteins; Nef, P24 and Tat (concentration of 10 nM each) conducted showing (a) I_{ds}–V_{gs} curve of the detection on the device. Enlarged graph in (b) shows the gate voltage shift value between HIV proteins; Nef, P24 and Tat and (c) shows the error bar of the gate voltage shift value for each protein (n=3). 115

Figure 4.27 Detection limit test has been conducted using 9 different concentrations from 0.2 nM, 0.4 nM, 0.6 nM, 0.8 nM, 1.0 nM, 5.0 nM, 10.0 nM, 100.0 nM and 1 µM showing (d) I_{ds}–V_{gs} curve of the different concentration detection on device and (e) V_{gs} shift of every protein concentration compared to control solution showing limit of detection obtained at 600 pM (n=3). 116

LIST OF ABBREVIATIONS

FET	Field effect transistor
IDE	Interdigitated electrode
SAW	Surface acoustic wave
GCE	Glassy carbon electrode
SPE	Screen printed electrode
JFET	Junction field effect transistor
MOSFET	Metal oxide semiconductor field effect transistor
MESFET	Metal semiconductor field effect transistor
BGFET	Back gate field effect transistor
ISFET	Ion sensitive field effect transistor
SGFET	Solution gate field effect transistor
DNA	Deoxyribonucleic acid
CNT	Carbon nanotube
MWCNT	Multiwalled carbon nanotube
SWCNT	Single walled carbon nanotube
POCT	Point of care testing
HIV	Human immunodeficiency virus
HIV-1	Human immunodeficiency virus type-1
HIV-2	Human immunodeficiency virus type-2
cDNA	Complementary deoxyribonucleic acid
RNA	Ribonucleic acid
WHO	World health organization
AIDS	Acquired immune deficiency syndrome
ELISA	Enzyme linked immunosorbent assay
SOI	Silicon on insulator
RIE	Reactive ion etching
LOD	Limit of detection
IUPAC	International Union of Pure and Applied Chemistry
IBM	International business machines
IC	Integrated circuit
CVD	Chemical vapor deposition
EDX	Energy dispersive X-ray
FTIR	Fourier transform infrared

TGA	Thermogravimetric analysis
TEM	Transmission electron microscope
XPS	X-ray photoelectron spectroscopy
SEM	Scanning electron microscope
AFM	Atomic force microscope
LB	Langmuir-blodgett
ZP	Zeta potential
Ig	Immunoglobulin
Fab	Fragment antigen-binding
SELEX	Systematic Evolution of Ligands by exponential enrichment
NMR	Nuclear magnetic resonance
EDC	1-Ethyl-3-(3-dimethylaminopropyl)carbodiimide
NHS	N-hydroxysuccinimide
APTES	(3-aminopropyl)triehoxysilane
GA	Glutaraldehyde
USA	United States of America
HTLV-III	Human T-cell lymphotropic virus-type III
LAV	Lymphadenopathy-associated virus
SIV	Simian immunodeficiency virus
DNA-PK	DNA-dependent protein kinase
FDA	Food and Drug Administration
RT	Reverse transcriptase
IN	Integrase
PR	Protease
SU	Surface
TM	Transmembrane
CA	Capsid
NC	Nucleosapsid
Tat	Trans-activator of transcription
Rev	Regulator of virion
Nef	Negative regulatory factor
Vpu	Viral protein u
Vif	Viral infectivity factor
Vpr	Viral protein r

QCM	Quartz crystal microbalance
SPR	Surface plasmon resonance
GNP	Gold nanoparticles
UV-Vis	Ultraviolet-visible
DI	Deionized water
BOE	Buffer oxide etch
IPA	Isopropanol
PR	Photoresist
UV	Ultraviolet
PVD	Physical vapour deposition
HPM	High performance microscope
fMWCNT	Functionalized multiwalled carbon nanotube
IR	Infrared
MW	Molecular weight
S1	Strand 1
S2	Strand 2
PAGE	Polyacrylamide gel electrophoresis
3D	Three dimension
SDS	Sodium dodecyl sulphate
TAR	Transactivation response

LIST OF SYMBOLS

π	Pi
nm	Nano meter
sp^2	One s and two p orbital
π-π	Pi-pi
COOH	Carboxyl
NH_3	Amine
SH	Thiol
F	Fluorine
OH	Hydroxyl
C=O	Carbonyl
HNO_3	Nitric acid
H_2SO_4	Sulfuric acid
$KMNO_4$	Potassium permanganate
H_2O_2	Hydrogen peroxide
$NaNO_2$	Sodium nitrite
HCl	Hydrochlorid acid
˚C	Degree celcius
rpm	Rotation per minute
ml	Millilitre
cm^2	Centimetre square
S	Siemens
cm	Centimetre
A	Adenosine
T	Thymine
U	Uracil
C	Cytosine
G	Guanine
ng	Nanogram
ppm	Parts per million
nM	Nanomolar
NaCl	Sodium chloride
Si	Silicon
NH_4OH	Ammonium hydroxide
SiO_2	Silicon oxide
µm	Micrometer

sccm	Standard cubic centimetre per minute
CF_4	Tetrafluoromethane gas
O_2	Oxygen gas
W	Watt
Pa	Pascal
Ni	Nickel
Au	Gold
M	Molar
mg	Milligram
KBr	Potassium bromide
K	Thousand
kV	Kilo volt
°	Degree
C	Carbon
O	Oxygen
mBar	Millibar
psi	Pound per square inch
wt%	Weight percent
v/v	Volume per volume
I_{ds}	Drain to source current
V_{ds}	Drain to source voltage
V_{gs}	Gate to source voltage
mM	Millimolar
KCl	Potassium chloride
pM	Picomolar
µM	Micromolar
NO_2^+	Nitronium ion
C=C	Carbon–carbon double bonds
C-C	Carbon–carbon single bonds
eV	Electron volts
V	Volt
mA	Milliampere
G	Conductance
I	Current
V	Voltage
SSA_{fMWCNT}	Specific surface area of MWCNT

SSA_{GS}	Surface specific surface area of graphene sheet
d_e	External diameter of MWCNT
n	Number of walls in MWCNT
d_{s-s}	Intershell distance in MWCNT
W_{fMWCNT}	Weight of MWCNT
$m^2\ g^{-1}$	Meter square per gram
m^2	Meter square
Amu	Atomic mass unit
kDa	Kilo dalton
TAR	Transactivation response
µl	Microlitre
mV	Millivolt
µA	Microampere

Pembangunan Karbon Nanotiub Berbilang Dinding Terintegrasi Transistor Kesan Medan Sebagai Biopenderia Protein HIV-1 Tat Bersensitiviti Tinggi

ABSTRAK

Virus kurang daya tahan imun (HIV) telah menjangkiti hampir 35 juta orang di seluruh dunia. Pelbagai ujian telah dibangunkan untuk mengesan kehadiran HIV semasa peringkat awal penyakit ini untuk mengurangkan risiko penyebaran ke manusia lain. Protein HIV-1 Tat adalah salah satu protein yang terdapat dalam HIV yang dilepaskan dengan banyak kira-kira 2 hingga 4 minggu selepas jangkitan. Pengesanan tahap awal penyakit boleh dicapai dengan mengesan protein Tat dalam individu berisiko tinggi. Ini mengurangkan risiko pandemik HIV. Transistor kesan medan dengan kawalan belakang (BGFET) telah dibangunkan untuk menjadi biosensor untuk pengesanan awal HIV. Protein Tat telah digunakan sebagai sasaran manakala untaian terpisah RNA aptamer telah dipilih sebagai prob pengesanan. Interaksi yang mengikat di antara untaian terpisah RNA aptamer dan protein HIV-1 Tat pada peranti biopenderia telah disahkan menggunakan ujian warna. Ujian ini berjaya menunjukkan interaksi berlaku antara untaian terpisah RNA aptamer dan HIV-1 Tat yang ditunjukkan oleh perubahan warna nanopartikel emas dari merah jambu kepada ungu. BGFET dibuat bersesuaian dengan molekul biologi menggunakan bahan nanokarbon seperti tiub karbon multi-dinding (MWCNT) sebagai tapak tetap biomolekul. Rawatan pengoksidaan menggunakan asid telah dijalankan untuk menambah kumpulan berfungsi kepada permukaan MWCNT dan kemudiannya dicirikan melalui mikroskop elektron pengimbasan pelepasan bidang (FESEM) dan X-ray difraksi (XRD). Analisa spektroskopi fotoelektron sinar-X (XPS) menunjukkan peningkatan ketara ~ 2.91% dalam kumpulan oksigen secara keseluruhan dan kenaikan ~ 1% diperhatikan pada kandungan karboksil terdiri daripada ikatan C = O dan O-C = O. Interaksi yang mengikat antara untaian terpisah RNA aptamer dan protein HIV-1 Tat dicirikan oleh analisis pengubah inframerah Fourier (FTIR) dan kuantifikasi elektrik isyarat semasa (Id) di atas voltan kawalan belakang (Vgs). Pencapaian had kepekaan interaksi antara aptamer dan HIV-1 Tat pada peranti yang dibuat adalah 600 pM. Untuk memastikan interaksi yang tulen dari aptamer dengan HIV-1 Tat, protein HIV-1 lain iaitu Nef dan p24 telah diinteraksikan dengan aptamer dan mereka memperlihatkan gangguan yang dapat diabaikan dengan peralihan voltan pintar 3.5 mV dan 5.7 mV, masing-masing menunjukkan signal yang 4 kali dan 2.5 kali lebih rendah daripada interaksi HIV-1 Tat.

Development of Multiwalled Carbon Nanotube Integrated Field Effect Transistor for Highly Sensitive HIV-1 Tat Protein Biosensor

ABSTRACT

Human immunodeficiency virus (HIV) has infected almost 35 million people worldwide. Various tests have been developed to detect the presence of HIV during the early stages of the disease in order to reduce the risk of transmission to other humans. The HIV-1 Tat protein is one of the proteins present in HIV that are released abundantly approximately 2 to 4 weeks after infection. Early stage detection of the disease can be achieved by detecting Tat protein in high risk individuals. This mitigates the risk of a HIV pandemic. A back gated field effect transistor (BGFET) has been developed to be a biosensor for the early detection of HIV. Tat protein has been used as the target while split RNA aptamer has been chosen as the detection probe. The binding interactions between split RNA aptamer and HIV-1 Tat protein on a biosensor device was validated using colorimetric assay. The assay successfully demonstrated the interaction occurred between split RNA aptamer and HIV-1 Tat indicated by the changes of gold nanoparticles color from pink to purple. BGFET was made biocompatible by using carbon nanomaterials like multiwalled carbon nanotube (MWCNT) as biomolecules immobilization site. Acid oxidation treatment was conducted to functionalize MWCNT with carboxyl functional groups and subsequently characterized through field emission scanning electron microscopy (FESEM) and X-ray diffraction (XRD). X-ray photoelectron spectroscopy (XPS) analysis had profound ~2.91% increment in overall oxygen group and ~1% increment was noticed with a specific carboxyl content owing to C=O and O–C=O bonding. The binding interaction between split RNA aptamer and HIV-1 Tat protein was characterized by Fourier transform infrared (FTIR) binding analysis and electrical quantification of current signal (I_{ds}) over a gate voltage (V_{gs}). The attainment of sensitivity with aptamer and HIV-1 Tat interaction on the fabricated device was 600 pM. To ensure the genuine interaction of aptamer with HIV-1 Tat, other HIV-1 proteins, Nef and p24 were interacted with aptamer and they displayed the negligible interferences with gate voltage shift of 3.5 mV and 5.7 mV, which shows 4 and 2.5 folds lesser than HIV-1 Tat interaction, respectively.

CHAPTER 1 : INTRODUCTION

1.1 Background

Implementing electronic devices as the medium for biological reaction detection has captivated great interest among researchers nowadays. The current trend of biosensing is moving towards the realization of point-of-care diagnostic systems which involve the integration of all the analytical stages on a single chip. Biosensor is an analytical device that utilizes biological component to act as molecular recognition unit. It combines the biological component and modern micro or nano electronic to form a powerful analytical tool for the application in pharmaceutical, medical, environmental and food analysis. There are a several devices that has been developed as biosensor such as field effect transistor (FET) (Bronder et al., 2015; Cheng et al., 2014; Rim et al., 2013), interdigitated electrode (IDE) (Azizah, Hashim, Gopinath, & Nadzirah, 2016; Huy et al., 2011; W. Zhang, Patel, Schexnider, Banu, & Radadia, 2014), surface acoustic wave (SAW) device (Crivianu-Gaita, Aamer, Posaratnanathan, Romaschin, & Thompson, 2015; Klauke, Gronewold, Perpeet, Plattes, & Petersen, 2013; Ten et al., 2016), glassy carbon electrode (GCE) (Moyo, Okonkwo, & Agyei, 2014; Pilehvar et al., 2014; Q. Wang, Zhang, Lin, & Weng, 2011), screen printed electrode (SPE) (Cavallini, Micheli, & Carrara, 2011; Hayat, Andreescu, & Marty, 2013; Kara et al., 2010) and etcetera. These portable and time-efficient devices are very efficient for rapid bacteria and virus detection hence reduce the analysis time, diagnose early and prevent epidemic of infectious disease.

FET is the most common device that has been developed for biosensing purposes due to its captivating ability which can quantify the field effect charges from biomolecules and translate it into a readable signal (Im, Huang, Gu, & Choi, 2007; D. S. Kim et al., 2003; Poghossian, Schultze, & Schöning, 2003; Veigas, Fortunato, & Baptista, 2015). FET has been developed as good and reliable biosensor with good sensitivity and selectivity (Dai, Gao, Lu, Li, & Wang, 2013a; Gao, Lu, Wang, & Li, 2016; Katsura, Yamamoto, Maehashi, Ohno, & Matsumoto, 2008; D.-S. Kim et al., 2004). The FET consists of a three-electrode system (source, drain and gate) and a channel. When supplied with voltage bias, electron will flow from drain to source via channel. The gate voltage supplied will either enhance or deplete the current flow through the channel. There are several type of FET that are available including junction field effect transistor (JFET), metal oxide semiconductor field effect transistor (MOSFET), metal semiconductor field effect transistor (MESFET), back gate field effect transistor (BGFET), ion sensitive field effect transistor (ISFET) / solution gate field effect transistor (SGFET) and etc. For biosensor purposes, deoxyribonucleic acid (DNA) or protein biomolecules interaction will be conducted at the surface channel as shown in Fig. 1.1. Deposition of material and immobilization of biomolecules taking place on the channel will result in changes in the electron density on the channel surface (Poghossian, Cherstvy, Ingebrandt, Offenhäusser, & Schöning, 2005). Any changes on the channel surface will be reflected on the drain current result (K. Y. Park, Kim, & Choi, 2005). With several modifications on the device using suitable material and proper surface modification, FET can provide a highly sensitive, rapid and label free detection.

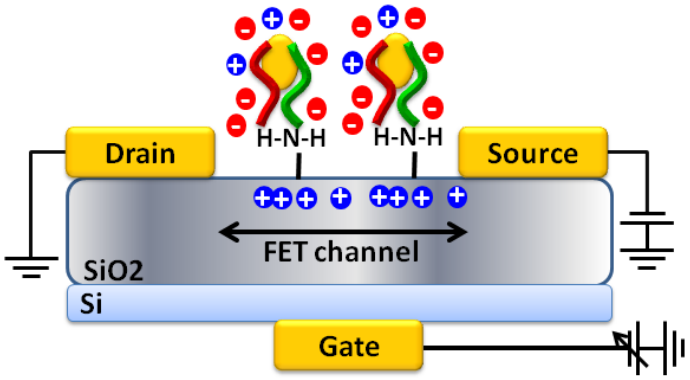

Figure 1.1 Schematic diagram of BGFET for DNA/protein biosensor.

A lot of studies have implemented the use of nanomaterial integrated with FET to function as an active site for biomolecules immobilization and reaction while optimizing its sensitivity. Carbon based materials are the material that have been used commonly on FET for the purpose of enhancing its signal. Carbon nanotube (CNT) is a biocompatible material that has been studied for integration with FET for biomolecules interaction sensing purposes. There are two types of CNT that is commonly used which are multiwalled carbon nanotube (MWCNT) and single walled carbon nanotube (SWCNT). CNT most intriguing characteristic that makes it a promising material in biosensor device is due to its long hollow tube structure with layers of wall made out of carbon ring that provide a huge surface area for interaction. Its surface can be functionalized to generate any types of functional groups for vast immobilization of biomolecules. Besides, its fast electron transfer kinetic enables it to convey the biological reaction signal effectively. There is abundance of research showing the fabrication of CNT-FET for highly sensitive biomolecules detection (Croce Jr, Vaddiraju, Chan, Seyta, & Jain, 2011; Maehashi et al., 2007; Oh et al., 2013; Pourasl et al., 2014; Stefansson, Kwon, & Ahn, 2012).